Hybrid spacecraft attitude control system

Renuganth Varatharajoo*, Ramly Ajir, Tamizi Ahmad
Department of Aerospace Engineering, University Putra Malaysia, 43400 UPM Selangor, Malaysia. *E-mail: renu99@gmx.de

ABSTRACT

The hybrid subsystem design could be an attractive approach for future spacecraft to cope with their demands. The idea of combining the conventional Attitude Control System and the Electrical Power System is presented in this article. The Combined Energy and Attitude Control System (CEACS) consisting of a double counter rotating flywheel assembly is investigated for small satellites in this article. Another hybrid system incorporating the conventional Attitude Control System into the Thermal Control System forming the Combined Attitude and Thermal Control System (CATCS) consisting of a "fluid wheel" and permanent magnets is also investigated for small satellites herein. The governing equations describing both these novel hybrid subsystems are presented and their onboard architectures are numerically tested. Both the investigated novel hybrid spacecraft subsystems comply with the reference mission requirements.

Keywords: Attitude Control Systems, Satellite Power, Temperature, Flow Control

NOMENCLATURE

K_w, K_P, K_I, K_D	control gains: proportional wheel gain [Nms/rad], proportional attitude gain [Nm/rad], integral attitude gain [Nm/s], derivative attitude gain [Nms/rad]
I_w, J_f, $I_{y,sat}$	wheel, fluid and satellite inertias [kgm^2]
$u = T_{attitude.cmd}$	proportional torque command [Nm]
T_{cmd}	attitude torque command [Nm]
$T_{energy.cmd}$	energy torque command [Nm]
T_D	external disturbamce torques exerted on the satellite [Nm]
T_y, T_s	torque exerted on the satellite [Nm]
$\theta_{ref.}$	reference satellite attitude [rad or deg]
$\theta_y, \theta_{sat.}$	true satellite attitudes [rad or deg]
Ω_{cmd}	wheel speed command [rad/s]
Ω_w	wheel speed [rad/s]
Ω_o	orbital frequency [rad/s]
Ω_f	fluid angular velocity [rad/s]
w_y, w_{sat}	attitude rates [rad/s]
l_θ	longitudinal length [m]

Δp_{loss}	friction pressure $f\frac{2\pi R}{D}\frac{\rho}{2}V^2$, [N/m²]
b	duct width [m]
B	magnetic flux density [T]
D	hydraulic diameter $\frac{2hb}{h+b}$ [m]
f	friction coefficient = 0.32 $Re^{-0.25}$
h	duct height [m]
V	fluid velocity [m/s]
Ha	Hartmann number $\sqrt{\frac{\sigma_{ec}}{\rho\nu}}Bh$
Re	Reynolds number = $\frac{VD}{\nu}$
ρ	density ($^{**}\rho = 5907$ kgm^{-3})
ν	kinematic viscosity ($^{**}\nu = 3.49 \times 10^{-7}$ m2 s^{-1})
σ_{ec}	electrical conductivity ($^{**}\sigma_{ec} = 3.7 \times 10^{6}$ Ohm-^{1}m^{-1})

**Gallium properties at 303 K.

1. INTRODUCTION

The requirements for the space missions in terms of their performances are gradually increasing. Therefore, spacecraft platforms have received attention in the recent years for a further optimisation. An approach would be to enhance the capabilities of each subsystem to keep the overall mass and volume budgets in the same level as today. Another idea would be to have novel hybrid subsystems onboard so that multi-tasking can be employed to a single subsystem. In doing so, the mass and volume budgets of a spacecraft platform could be decreased, and therefore, allowing the spacecraft payload mass increment. The space flywheels are much more promising than the conventional electrochemical batteries as an energy storage device because of their higher depth-of-discharge, longer life cycle and temperature independence. Additionally, these flywheels can be employed for the spacecraft attitude control as well. Such a concept was investigated for larger spacecraft [1, 2]. Instead, Renuganth and Fasoulas have proposed the hybrid concept for small satellites [3]. In addition, they have proposed another hybrid attitude control system that couples the attitude and thermal control tasks for small satellites [4]. The novelty in this paper lies in the attitude performance comparison of the two novel hybrid subsystems for small satellites, i.e., the Combined Energy and Attitude Control System (CEACS) and the Combined Attitude and Thermal Control System (CATCS).

2. CEACS

The CEACS consists of two counter rotating high speed composite rotors, motor/generators, magnetic bearings and control electronics [3]. The complete system can be mounted along the pitch axis so that a bias speed along the pitch channel can provide a roll/yaw passive stiffness. The CEACS onboard control architecture based on a PD type attitude controller is

presented in Figure 1. Note that each flywheel is controlled by a proportional controller K_W, and it operates in the speed mode. Denoting s the Laplace, the flywheel speed loop yields

$$\frac{\Omega_w}{\Omega_{cmd}} = \frac{1}{1+\tau_w s} \tag{1}$$

whereby the loop delay is

$$\tau_w = \frac{I_w}{K_w k_m} \tag{2}$$

For an identical double flywheel system, the torque compartment simplifies to

$$\frac{T_y}{T_{cmd}} = \frac{2KI_w}{1+\tau_w s} \tag{3}$$

Assuming that the roll/yaw inertias are similar ($I_x \approx I_z$), the term incorporating the orbital frequency Ω_o is negligible. Consequently, the pitch axis dynamics yields

$$\frac{\theta_y}{\theta_{ref.}} = \frac{1}{1+\frac{K_D}{K_P}s+\frac{I_y}{K_P}s^2+\frac{I_y\tau_w}{K_P}s^3} \tag{4}$$

The external disturbances influence the pitch attitude according to

$$\frac{\theta_y}{T_D} = \frac{1+\tau_w s}{K_P+K_D s+I_y s^2+\tau_w I_y s^3} \tag{5}$$

In Figure 1 the energy command $T_{energy,cmd}$ is simultaneously issued by the bus voltage regulator. The energy command is proportional to the available solar power (charging phase), and the payload power demand (discharging phase). The bus architecture developed by Renuganth and Tarmizi is adopted in this investigation [5]. It should be pointed out that the bus voltage regulation is managed by a separate loop, which operates at a higher frequency (e.g. 100 Hz). In this way, the onboard power management does not interfere with the satellite attitude management that operates at a lower frequency (e.g. 0.1 Hz).

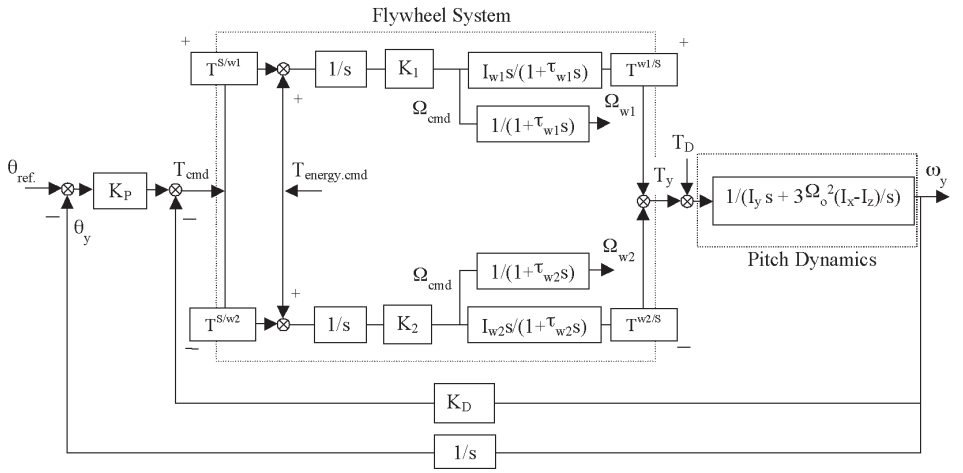

Figure 1 CEACS control architecture. $T^{S/w1}$ and $T^{w1/S}$ are the projection matrixes with a scalar value of 1. And, $T^{S/w2}$ and $T^{w2/S}$ have a scalar value of –1. The moments of inertia for both flywheels and the corresponding time constants, and the other constants are held equal, i.e., $k_m = k_{m2} = k_m = 1$, $I_{w1} = I_{w2} = I_w = 15.5 \times 10^{-3}$ kgm^2, $K_1 = K_2 = K = 0.5$ and $\tau_{w1} = \tau_{w2} = \tau_w = 2$s. Also, let $2\,K\,k_m = 1$ and the pitch axis moments of inertia $I_y = 16.9$ kgm^2.

2.1 THE CEACS ONBOARD PERFORMANCES

A reference mission is proposed for the numerical performance evaluation as follows: 100 kg satellite with $1 \times 1 \times 1$ m^3 of volume, 5 years of mission duration, a circular orbit at 500 km with an inclination of 53°, pitch axis attitude requirement $< 0.2°$, and 98 W of power requirement [4]. The CEACS should store about 60 Wh of energy to fulfil the reference mission's energy demand during the eclipse phase. The external disturbance torques is $T_D = 3.34 \times 10^{-5}$ Nm + 2.81×10^{-5} (sin Ω_ot) Nm. The flywheels are mounted on the pitch axis of the satellite and are requested not only to keep the pointing accuracy of the axis below 0.2° but also to provide a minimum bias speed of about 370 rad/s for the roll/yaw axis stiffness. Therefore, the initial speed for one of the flywheels is set to 1000 rad/s in the numerical simulation (Matlab®-Simulink™). The proportional and derivative attitude control gains are $K_P = 0.0327$ Nm/rad and $K_D = 0.9489$ Nms/rad, respectively. The charge/discharge efficiency is kept to about 80 %, and a depth of discharge of about 90 % is maintained in the numerical treatment. In Figures 2 (a) and (b), the required attitude accuracy and energy (≈ 60 Wh) during the eclipse phase is fulfilled by the CEACS. The flywheels' speeds increase during the charging phase and decrease during the discharging phase, shown in Figure 2 (c). Figure 2 (d) shows the needed bias speed along the pitch axis is available. It is worthwhile to point out that these performances can be still maintained in the face of imperfect knowledge of CEACS system parameters, and the mass/volume savings can also be achieved; see Refs. 3 and 6, respectively.

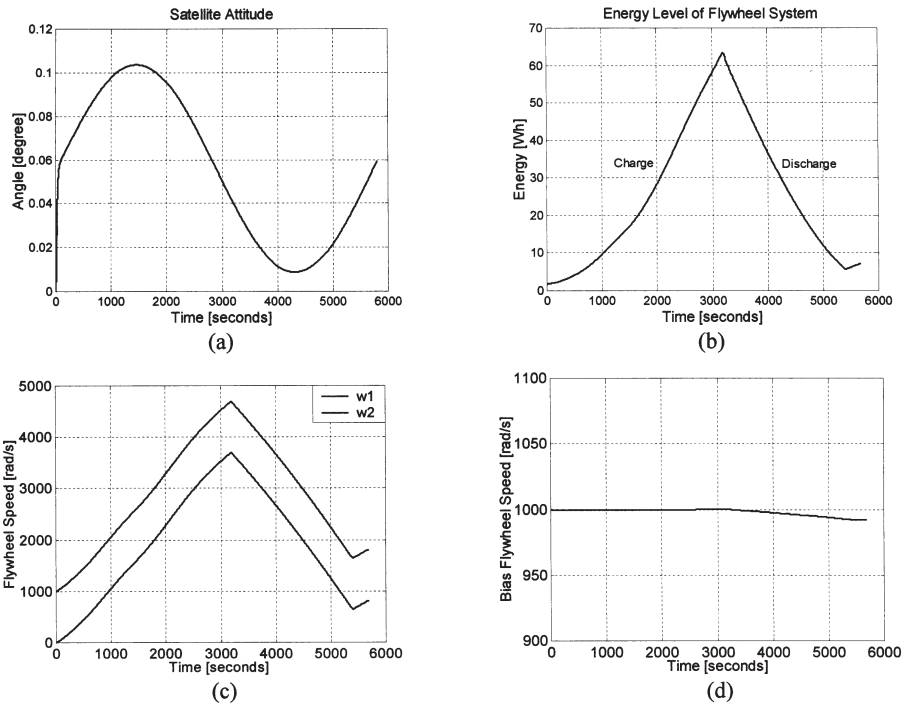

Figure 2 The CEACS onboard performances

3. CATCS

The Combined Attitude and Thermal Control System (CATCS) couples an existing onboard temperature gradient with the magnetohydrodynamic (MHD) effects for its operation. An excess onboard heat could be used by the CATCS for the spacecraft attitude and thermal management. As a result, the power budget for these tasks could be suppressed. The CATCS is proposed mainly for satellites that require active thermal controllers. The basic idea to combine the thermal control system and the attitude control system is by utilizing an electrical conductive fluid, which circulates in a closed loop to serve as a "heat conductor" and a "momentum generator". Thus, the conventional heat pipes could be replaced by a duct system in which the fluid with a reasonable heat transfer coefficient circulates, and simultaneously generates reaction torques for the attitude control. The fluid motion could be influenced by a variation of the external and internal effects, e.g., electric and magnetic fields, and temperature gradients. The concept makes use of the existing temperature gradient in satellites to create a flow through the coupling of the thermoelectric and magnetic fields. The thermoelectric current can be generated by the temperature gradient between metal pairs. Hence, when a magnetic field is introduced near the generated electric current, a fluid flow is induced. The system details are given in Figure 3 (a). Two configurations are proposed for CATCS; see Figures 3 (b) and (c). The former benefits from the internal heat sources (e.g. payloads) and the latter benefits from an external heat source (e.g. Sun). These configurations allow an active heat dissipation to the neighbouring satellite

walls, which will eventually avoid thermal stresses on the satellites. Additionally, this method is independent from the natural convection phenomena, and therefore enhances the heat transport activity.

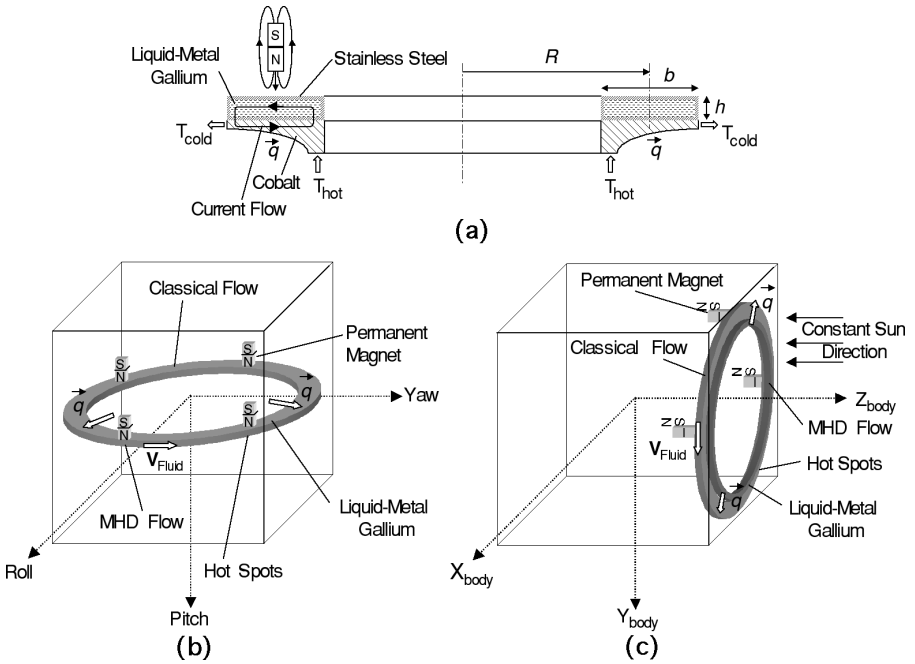

Figure 3 The CATCS setup. Radius R = 0.5 m, height h = 5 mm, width b = 20 mm, mass m = 1.86 kg, MHD pumps n = 4, fluid inertia J_f = 0.46 kgm^2, and heat flow q.

In both configurations, the fluid velocity is controlled by varying the distance between the permanent magnets and the fluid housing. This task can be executed by engaging the linear motors to position the magnets. The working fluid selected is gallium, which has a melting point at 303 K. In fact, this value can be easily dropped by adding the indium (24 %) and tin (16 %) compounds. The thermoelectric generator selected as an example is cobalt with an absolute thermoelectric power ΔS of about -35 μV/K. Since the liquid-metal gallium is active towards cobalt, the stainless steel is chosen for the fluid housing. Both the materials, gallium and stainless steel, have no absolute thermoelectric powers, but they are reasonable heat and electric conductors. The permanent magnets chosen for the setup are Neodymium-Iron-Boron ($Nd_2Fe_{14}B$) type. The crucial parameter to be estimated first is the maximum fluid velocity V_{max}. The CATCS working principle is that the pressure drop due to the duct friction Δp_{loss} must be balanced by the total pressure of the magnetohydrodynamics (MHD) pumps $n\Delta p_{pump}$. Hence, the Bernoulli's equation for this closed fluid system yields

$$\Delta p_{loss} = n \Delta p_{pump} \tag{6}$$

The equivalent pressure provided by a MHD pump is induced by the Lorentz force F_L (F_L = $b\ I\ B$) over a cross section A (A=$h\ b$).

$$\Delta p_{pump} = \frac{F_L}{A} \tag{7}$$

Solving Eq. (6), the fluid velocity yields

$$V = \left(\frac{n I B D^{1.25}}{0.32 b \nu^{0.25} \pi R \rho} \right)^{\frac{4}{7}} \tag{9}$$

The generated thermoelectric current I_{local} is

$$I_{local} = \sigma_{ec} \frac{A_e}{b} \Delta S \, \Delta T \, , \tag{10}$$

where the cross section A_e the mean circumference of duct l_f times height h. It is assumed that a MHD compartment has a particular length $l_f \approx 0.05$ *m*. Subsequently, the estimated current is about 80 A corresponding to an assumed system temperature gradient ΔT of 50 K. It is important to note that the current magnitude is for a single horizontal field; hence, the current total current density (A/m^2) is deemed to be lower. For the magnetic flux density $B = 0.5$ *T*, Eq. (9) yields for the maximum fluid velocity $V_{max} = 1.07$ *m/s*. As a result, the corresponding angular momentum is about 0.95 Nms. The CATCS will be used as "fluid reaction wheel" as well with an estimated response time of less than 2 s for a Hartmann number $Ha >> 1$ [4].

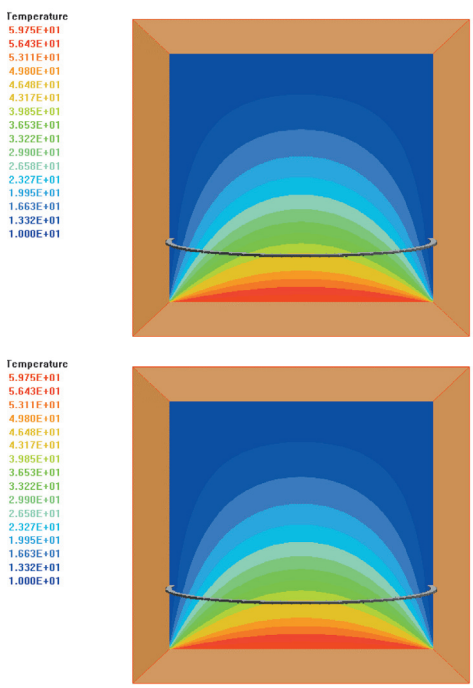

Figure 4 Satellite thermal compartment

3.1 THE CATCS ONBOARD PERFORMANCES

The reference mission in the preceding section for the CEACS testing is retained for the CATCS numerical treatment. Having calculated the fluid flow velocity, the satellite thermal compartment can be modelled using the Phoenics^{TM} software. As an example, the configuration in Figure 3 (b) is chosen for the thermal modelling. Figures 4 (a) and (b) show the temperature distributions in the satellite and in the CATCS setup, respectively. The maximum and minimum temperatures are between 60∞C and 10∞C. Therefore, the satellite onboard thermal compartment can be regulated.

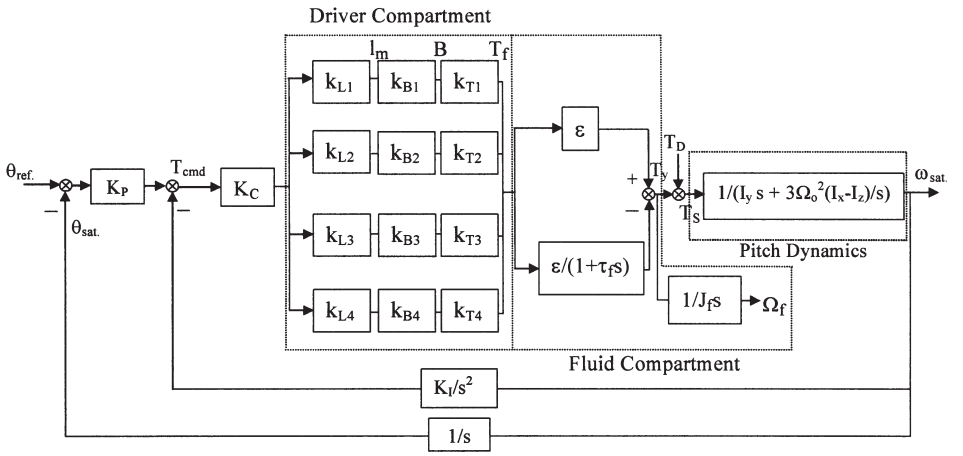

Figure 5 The CATCS onboard architecture

In order to induce an attitude control torque, the fluid velocity is controlled by varying the distance between the permanent magnets and the fluid housing. This task can be executed by engaging the linear motors to position the magnets the fluid housing. This task can be executed by engaging the linear motors to position the magnets vertically. The CATCS control architecture is presented in Figure 5, whereby d the displacement, B the induced magnetic flux density and T_f the resulting torque are the physical constants describing the driver. Their dependencies are given by the linear motor constant k_L, the induced flux density constant k_B and the resulting torque constant k_T, respectively. The system gains are: $K_C = 1/n$, and all the drivers' constants are held constant. The product of these constants is defined as: $k_L \times k_B \times k_T = k_G$. And, the ε in Figure 5 represents the system torque accuracy: $\varepsilon = 1 \pm \varepsilon_T$, whereby ε_T the internal torque gain errors.

For an ideal system, ε_T would be equal to zero so that $\varepsilon = 1$. The attitude controller selected is a PI type, which fulfils the stability aspects as well. The satellite inertias are taken equal, e.g., 16.9 kgm^2. Hence, the pitch attitude channel dynamics yields

$$\frac{\theta_{sat.}}{\theta_{ref.}} = \frac{1}{\left(1 + \frac{K_P}{K_i}s + \frac{I_y}{K_i k_G \tau_f}s^2 + \frac{I_y}{K_i k_G}s^3\right)} \tag{11}$$

On the other hand, the pitch channel's attitude disturbance yields

$$\frac{\theta_{sat.}}{T_D} = \frac{1+\tau_f s}{\tau_f J_{sat.} s^3 + J_{sat.} s^2 + \tau_f K_P k_G s + \tau_f K_i k_G} \tag{12}$$

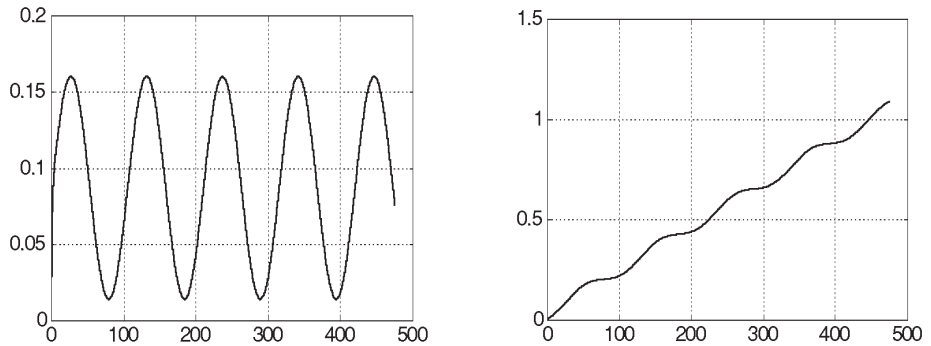

Figure 6 The CATCS onboard performances

The CATCS control architecture in Figure 5 is amenable to the numerical treatments (Matlab®,-Simulink™) for the attitude performance analysis. The chosen attitude control gains are $K_P = 0.8$ *Nm/rad* and $K_I = 0.011$ *Nm/s*, and k_G is regarded as unity so that the desired and exerted torque commands are directly proportional. The system's response time τ_f was set to 2 s. And, the linear motors' delays (e.g. 50 ms) were also considered in the simulation. The CATCS performance simulation results are depicted in Figures 6 (a) and (b). The pitch attitude is within the satellite's attitude pointing budget ($\theta_{sat.} < 0.2°$) in Figure 6 (a). The fluid velocity attains the maximum velocity after about 5 operational orbit periods; see Figure 6 (b). In the face of imperfect knowledge of CATCS system parameters, the system still fulfils the mission and the mass/volume savings can be achieved as well [4].

4. CONCLUSIONS

All the relevant mathematical models describing both the hybrid subsystems and their onboard architectures are implemented. Subsequently, the numerical treatments are performed to evaluate the performance of the developed architecture for a selected reference mission. The subsystems comply with the requirements of the reference mission. In fact, their attitude performances are comparable. Therefore, the selection of these hybrid subsystems is for a particular space mission mainly governed by the spacecraft platform design. In this regards, commissioning these hybrid subsystems onboard the future spacecraft platforms would benefit the space missions, i.e., life and performance enhancement, mass and volume savings, etc.

REFERENCES

1. Barde, H., Energy Storage Wheel Feasibility Study, *Proceedings of 4th Tribology Forum and Advances in Space Mechanisms*, No. 10, European Space Agency, Noordwijk, The Netherlands, 2001, 1-26.

2. Guyot, P., Barde, H. and Griseri, G.. Flywheel Power and Attitude Control System (FPACS), *Proceedings of 4th ESA Conference on Spacecraft Guidance, Navigation and Control System,* No. ESA-SP-425, European Space Agency, Noordwijk, The Netherlands, 1999, 371-378.

3. Renuganth, V. and Fasoulas, S., Methodology for the Development of Combined Energy and Attitude Control Systems for Satellites, *Aerospace Science & Technology*, 2002, **6**, 303-311.

4. Renuganth, V., Kahle, R. and Fasoulas, S., Approach for Combining Attitude and Thermal Control Systems, *Journal of Spacecraft and Rockets,* 2003, **40**, 657-664.

5. Renuganth, V. and Tarmizi, M., Flywheel Energy Storage for Spacecraft, *Journal of Aircraft Engineering and Aerospace Aerospace Technology*, 2004, **76**, 384-390.

6. Renuganth, V. and Kahle, R., A Review of Spacecraft Conventional and Synergistic Systems, *Journal of Aircraft Engineering and Aerospace Technology*, 2005, **77**, 131-141.